

RAPID COMMUNICATION

A simple rule for finding Dirac cones in bilayered perovskites^{*}

Recent citations

- [B. Venkata Shiva Reddy et al](#)

To cite this article: Xuejiao Chen *et al* 2019 *Chinese Phys. B* **28** 077106

View the [article online](#) for updates and enhancements.

A simple rule for finding Dirac cones in bilayered perovskites*

Xuejiao Chen(陈雪娇)^{1,2}, Lei Liu(刘雷)^{1,†}, and Dezhen Shen(申德振)^{1,‡}¹State Key Laboratory of Luminescence and Applications, Changchun Institute of Optics, Fine Mechanics and Physics, Chinese Academy of Sciences, Changchun 130033, China²University of Chinese Academy of Sciences, Beijing 100049, China

(Received 31 May 2019; published online 5 June 2019)

A simple rule for finding Dirac cone electronic states in solids is proposed, which is neglecting those lattice atoms inert to particular electronic bands, and pursuing the two-dimensional (2D) graphene-like quasi-atom lattices with s- and p-bondings by considering the equivalent atom groups in the unit cell as quasi-atoms. Taking CsPbBr₃ and Cs₃Bi₂Br₉ bilayers as examples, we prove the effectiveness and generality of this rule with the density functional theory (DFT) calculations. We demonstrate that both bilayers have Dirac cones around the Fermi level and reveal that their corresponding Fermi velocities can reach as high as $\sim 0.2 \times 10^6$ m/s. This makes these new 2D layered materials very promising in making new ultra-fast ionic electronic devices.

Keywords: Dirac cone, perovskites, graphene, density functional theory**PACS:** 71.15.Mb, 73.22.Pr**DOI:** 10.1088/1674-1056/28/7/077106

1. Introduction

Dirac cone describes the gapless linear-dispersion of electronic bands and characterizes the superior ballistic massless charge-carrier transport of solids, such as in graphene^[1–3] or on the surfaces of topological insulators.^[4–6] Theoretically, Dirac cones were predicted in 1947 in graphene, whose honeycomb lattice of s-p bonding results in a conical band structure with the linearly dispersive valence and conduction bands touching each other at the Dirac points (K or K') of its hexagonal Brillouin zone.^[1] Nevertheless, it was only after its first isolation^[7] that graphene has become a source of new sciences, and aroused research upsurges again and again over its novel electronic behaviors.^[8–20] In fact, by energy-band theory and symmetry analysis,^[1] the normal Dirac cones as presented in graphene will generally appear in those materials, as long as they have a similar honeycomb bonding style as graphene. However, among hundreds of two-dimensional (2D) materials examined by now, only graphynes,^[21] silicene and germanene,^[22] ionic boron,^[23] and others^[24] have been identified to be the normal Dirac materials. Nevertheless, unlike graphene, these 2D Dirac materials are made of some sort of artificial lattices where the atoms do not bond together as they do in their stable natural structural polymorphs. In this paper, we propose that following a simple but effective rule, more Dirac cone states can generally be found in the 2D materials with stable natural bonding structures.

Here, perovskites are selected to demonstrate the physics behind the rule we have proposed for finding 2D Dirac materials. As shown in Fig. 1(a), normally, perovskites have

the well-known ABX_3 lattice structure, where the 6-fold coordinated B cation and its surrounded X anions form the BX_6 octahedron, the BX_6 octahedra share their X corners to form the three-dimensional (3D) skeleton, and the A cations occupy each hole among the 8 BX_6 octahedra. For a cubic ABX_3 lattice, if viewed from the $[111]$ direction, it natively presents hexagonal symmetry as shown in Fig. 1(b). While the A cations stay isolated from the BX_6 skeleton, their electronic states normally do not participate in forming the low-energy bands dispersing near the Fermi level. For a selected halide perovskite (CsPbBr₃), figure 1(c) plots its gapped electronic band structure calculated with density functional theory (DFT), together with the total and site-decomposed density of states (DOSs). It demonstrates clearly that the electronic orbitals of the A cations stay a few electronvolts away from the valence band maximum (VBM) and the conduction band minimum (CBM), thus playing no role in deciding the low-energy electronic behaviors of a perovskite.^[25,26] Therefore, for those low energy charge carriers, regardless of electrons or holes, propagating in a perovskite crystal, the effective lattice they see would be without A cations, as shown in Fig. 1(d). For such a cubic lattice, if sliced out along the (111) plane, two BX_6 layers naturally construct the hexagonal honeycomb lattice with two equivalent BX_6 sublattices similar to graphene, as shown in Fig. 1(e). If considering the BX_6 octahedron as a quasi-atom, such a BX_6 bilayer transforms into a buckled single quasi-atom layer with exactly the same structure as silicene,^[22] as shown in Fig. 1(f).

*Project supported by the National Natural Science Foundation of China (Grant No. 61525404).

†Corresponding author. E-mail: liulei@ciomp.ac.cn

‡Corresponding author. E-mail: shendz@ciomp.ac.cn

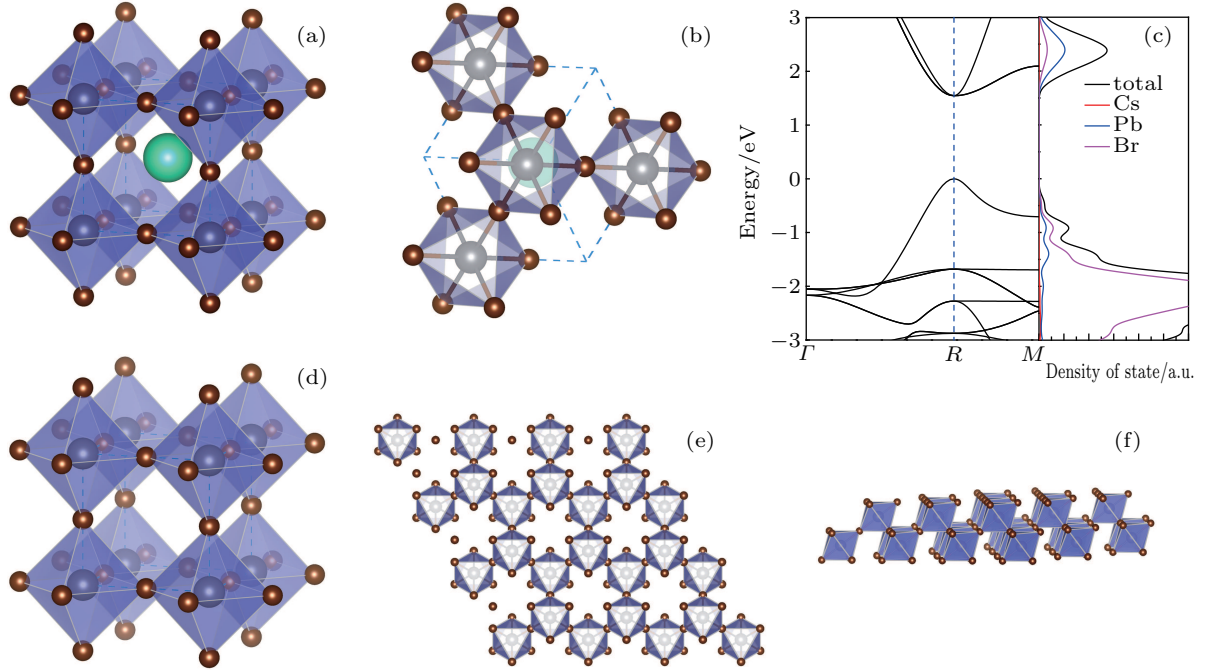


Fig. 1. (a) The crystal structure of a cubic ABX_3 perovskite, where the green, gray, and brown balls represent the A cations, B cations, and the X anions, respectively; (b) the crystal structure of a cubic perovskite viewed from its $[111]$ direction; (c) the calculated electronic band structure of bulk $CsPbBr_3$, together with its total and site-decomposed DOS; (d) the effective crystal structure of a cubic ABX_3 perovskite effectively seen by its low energy charge carriers; (e) the top view of the crystal structure of a BX_6 bilayer sliced out along the (111) plane of a cubic perovskite, which constructs the hexagonal honeycomb lattice with two equivalent BX_6 sublattices; and (f) the side view of the crystal structure of a hexagonal BX_6 bilayer, which indeed presents a buckled single quasi-atom (BX_6) layer.

Consequently, a hexagonal perovskite bilayer will naturally present the Dirac-cone electronic states as the graphene at its Dirac points of K and K' . This is a corollary based on the honeycomb symmetry of BX_6 sublattices and the s- and p-binding characters of BX_6 octahedra.^[1] As a verification example, the hexagonal $CsPbBr_3$ bilayer is selected to calculate its electronic band structures near the Fermi level. Here, the DFT calculations are performed within the Perdew–Burke–Ernzerhof (PBE) generalized gradient approximation^[27] and the projected augmented wave (PAW) method,^[28] as implemented by the Vienna *ab initio* simulation package (VASP).^[29–31] The cutoff energy for the plane-wave basis set is 300 eV and the Brillouin zone is sampled with the Monkhorst–Pack mesh of $6 \times 6 \times 6$ for bulk and $6 \times 6 \times 1$ for bilayer $CsPbBr_3$. The lattice parameter of bulk $CsPbBr_3$ is set to its experimental value $a_0 = 5.874$ Å.^[32] For the $CsPbBr_3$ (111) bilayer, it has the lattice constant of 8.307 Å ($\sqrt{2} \times 5.874$ Å) and the thickness of about 6.783 Å.

As expected, as shown in Fig. 2, its top valence and bottom conduction bands disperse linearly and touch each other at K and K' points. Their orbital-decomposed DOS clearly reveals the s- and p-orbital nature of both bands around the Dirac points, and this is further evidenced by the insets of Fig. 2 which plot the isosurfaces of VBM and CBM partial charge densities. By fitting these two bands at $\mathbf{k} = \mathbf{K} + \mathbf{q}$ to the expression $v_F \simeq E(\mathbf{q})/\hbar|\mathbf{q}|$,^[22] the Fermi velocity is estimated to be $v_F \sim 0.2 \times 10^6$ m/s, which is one fifth of v_F of graphene. While graphene has the intrinsic carrier mobil-

ity of 2×10^5 $\text{cm}^2 \cdot \text{V}^{-1} \cdot \text{s}^{-1}$,^[33] it is reasonable to infer that the carrier mobility in such a $CsPbBr_3$ bilayer may go around 4×10^4 $\text{cm}^2 \cdot \text{V}^{-1} \cdot \text{s}^{-1}$. This makes it rather superior in making ultra-fast electronic devices in comparison with those conventional semiconductors^[34] which normally have mobilities less than 10^4 $\text{cm}^2 \cdot \text{V}^{-1} \cdot \text{s}^{-1}$.

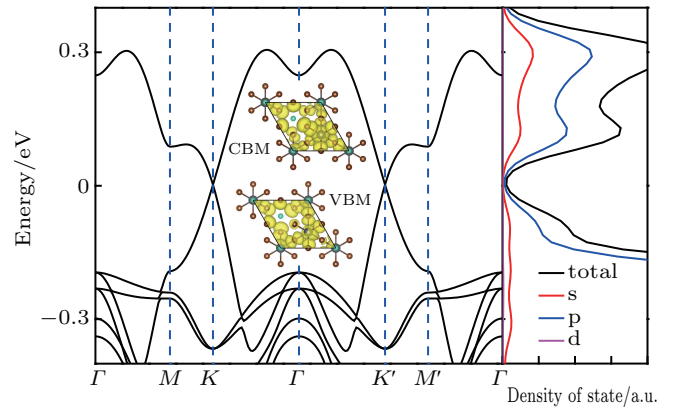


Fig. 2. The calculated electronic band structure of a hexagonal $CsPbBr_3$ bilayer (the insets plot the isosurfaces of VBM and CBM partial charge densities), together with its orbital-decomposed DOS.

Moreover, the vacancy-order halide perovskites $A_3B_2X_9$ (A : Cs; B : Fe, Sb, or Bi; X : Cl, Br, or I) are selected to demonstrate the effectiveness of this rule to find the Dirac electronic states away from the Fermi level. Naturally, the $A_3B_2X_9$ perovskites are stacked together by those bilayers of linked BX_6 octahedra. Figures 3(a) and 3(b) present the crystal structure of $Cs_3Bi_2Br_9$ as an example of the vacancy-order

halide perovskites. If viewed from their natural hexagonal axis, the $A_3B_2X_9$ perovskites present the honeycomb lattice of BX_6 quasi-atoms, as shown in Fig. 3(c). Experimentally, in 1977, the bulk $Cs_3Bi_2Br_9$ crystals were successfully grown by dissolving $Bi(OH)_3$ and Cs_2CO_3 in a dilute HBr solution by Lazarini *et al.*^[35] This layered material exhibits trigonal symmetry with a space group of $P\bar{3}m1$ and lattice constants of $a = 7.972 \text{ \AA}$ and $c = 9.867 \text{ \AA}$.^[35] As a stacking unit, its bilayer is inherently stable as graphene to graphite or single-layer h-BN to bulk h-BN. Based on the similar quasi-atom analysis on the $CsPbBr_3$ bilayer, the $Cs_3Bi_2Br_9$ bilayer will certainly present the Dirac electronic states as well.

Figure 3(d) shows the calculated electronic band structure of the $Cs_3Bi_2Br_9$ bilayer. And as expected, it presents

the crossing Dirac bands as well. However, as Bi contributes one more electron in $Cs_3Bi_2Br_9$ than Pb does in $CsPbBr_3$, its Fermi level goes above the Dirac bands for the $Cs_3Bi_2Br_9$ bilayer. Its Fermi velocity at the crossing point is found to be $v_F \sim 0.2 \times 10^6 \text{ m/s}$, which equals the value of the $CsPbBr_3$ bilayer. Furthermore, as the layer interaction is rather weak in bulk $Cs_3Bi_2Br_9$, its electronic band structure exhibits similar Dirac bands below the Fermi level, as shown in Fig. 3(e). It is notable that the electronic band structures of $A_3B_2X_9$ perovskites have been previously calculated, such as on $Cs_3Bi_2Br_9$,^[36] or on $Cs_3Sb_2I_9$.^[37] However, in these studies, the Dirac-band features of their band structures were neither noticed nor pointed out.

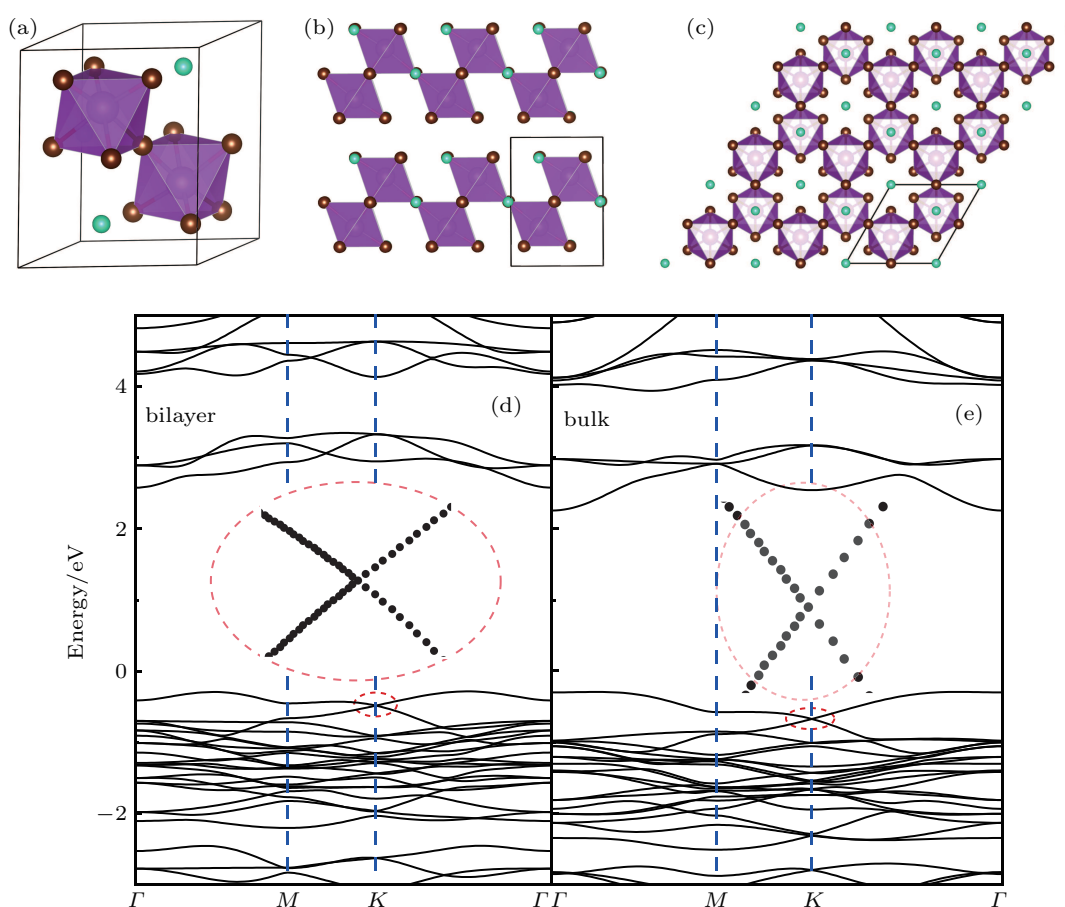


Fig. 3. The crystal structures of $Cs_3Bi_2Br_9$ (a) in its primitive cell, (b) from the side view, and (c) from the top view along its natural hexagonal axis, and the calculated electronic band structures of (d) bilayer and (e) bulk $Cs_3Bi_2Br_9$, where the insets zoom in their Dirac bands below the Fermi level.

In conclusion, we propose a quasi-atom rule for searching 2D Dirac materials in the conventional solids with natural stable bonding lattices. With this rule, we demonstrate with DFT calculations that hexagonal perovskite ABX_3 bilayers, such as the $CsPbBr_3$ (111) bilayer, may have the Dirac band crossing at the Fermi level. Similarly, taking $Cs_3Bi_2Br_9$ as an example, we further demonstrate that the hexagonal vacancy-order halide perovskite $A_3B_2X_9$ bilayers, together with their bulk

phases, will have the Dirac bands below the Fermi level. Both $CsPbBr_3$ and $Cs_3Bi_2Br_9$ bilayers exhibit the Fermi velocity of $\sim 0.2 \times 10^6 \text{ m/s}$, which makes them promising in making ultra-fast electronic devices.

References

- [1] Wallace P R 1947 *Phys. Rev.* **71** 622
- [2] Novoselov K S, Geim A K, Morozov S V, Jiang D, Katsnelson M I,

- Grigorieva I V, Dubonos S V and Firsov A A 2005 *Nature* **438** 197
- [3] Zhang Y B, Tan Y W, Stormer H L and Kim P 2005 *Nature* **438** 201
- [4] Bernevig B A, Hughes T L and Zhang S C 2006 *Science* **314** 1757
- [5] Hsieh D, Qian D, Wray L, Xia Y, Hor Y S, Cava R J and Hasan M Z 2008 *Nature* **452** 970
- [6] Chen Y L, Analytis J G, Chu J H, Liu Z K, Mo S K, Qi X L, Zhang H J, Lu D H, Dai X, Fang Z, Zhang S C, Fisher I R, Hussain Z and Shen Z X 2009 *Science* **325** 178
- [7] Novoselov K S, Geim A K, Morozov S V, Jiang D, Zhang Y, Dubonos S V, Grigorieva I V and Firsov A A 2004 *Science* **306** 666
- [8] Geim A K and Novoselov K S 2007 *Nat. Mater.* **6** 183
- [9] Geim A K 2009 *Science* **324** 1530
- [10] Neto Castro A H, Guinea F, Peres N M R, Novoselov K S and Geim A K 2009 *Rev. Mod. Phys.* **81** 109
- [11] Brumfiel G 2009 *Nature* **458** 390
- [12] Service R F 2009 *Science* **324** 875
- [13] Editorial 2010 *Nat. Nanotech.* **5** 755
- [14] Kim P 2010 *Nat. Mater.* **9** 792
- [15] Novoselov K S, Falcko V I, Colombo L, Gellert P R, Schwab M G and Kim K 2012 *Nature* **490** 192
- [16] Service R F 2015 *Science* **348** 490
- [17] Gibney E 2018 *Nature* **555** 151
- [18] Cao Y, Fatemi V, Fang S, Watanabe K, Taniguchi T, Kaxiras E and Jarillo-Herrero P 2018 *Nature* **556** 43
- [19] Xu Q, Ma T, Danesh M, Shivanianju B N, Gan S, Song J, Qiu C W, Cheng H M, Ren W and Bao Q 2017 *Light Sci. Appl.* **6** e16204
- [20] Zheng Z B, Li J T, Ma T, Fang H L, Ren W C, Chen J, She J C, Zhang Y, Liu F, Chen H J, Deng S Z and Xu N S 2017 *Light Sci. Appl.* **6** e17057
- [21] Malko D, Neiss C, Vines F and Gorling A 2012 *Phys. Rev. Lett.* **108** 086804
- [22] Cahangirov S, Topsakal M, Akturk E, Sahin H and Ciraci S 2009 *Phys. Rev. Lett.* **102** 236804
- [23] Ma F, Jiao Y, Gao G, Gu Y, Bilic A, Chen Z and Du A 2016 *Nano Lett.* **16** 3022
- [24] Wang J, Deng S, Liu Z and Liu Z 2015 *Nat. Sci. Rev.* **2** 22
- [25] Chen X J, Hand D, Su Y, Zeng Q H, Liu L and Shen D Z 2018 *Phys. Status Solidi RRL* **12** 1800193
- [26] Chen X J, Liu L and Shen D Z 2018 *J. Phys.: Condens. Matter* **30** 265501
- [27] Perdew J P, Burke K and Ernzerhof M 1996 *Phys. Rev. Lett.* **77** 3865
- [28] Blochl P E 1994 *Phys. Rev. B* **50** 17953
- [29] Kresse G and Furthmuller J 1996 *Comput. Mater. Sci.* **6** 15
- [30] Kresse G and Furthmuller J 1996 *Phys. Rev. B* **54** 11169
- [31] Kresse G and Joubert D 1996 *Phys. Rev. B* **54** 11169
- [32] Moller C K 1958 *Nature* **182** 1436
- [33] Morozov S V, Novoselov K S, Katsnelson M I, Schedin F, Elias D C, Jaszczak J A and Geim A K 2008 *Phys. Rev. Lett.* **100** 016602
- [34] Yettapu G R, Talukdar D, Sarkar S, Swarnkar A, Nag A, Ghosh P and Mandal P 2016 *Nano Lett.* **16** 4838
- [35] Lazarini F 1977 *Acta Cryst.* **B33** 2961
- [36] Bass K K, Estergreen L, Savory C N, Buckeridge J, Scanlon D O, Djurovich P I, Bradforth S E, Thompson M E and Melot B C 2017 *Inorg. Chem.* **56** 42
- [37] Singh A, Boopathi K M, Mohapatra A, Chen Y F, Li G and Chu C W 2018 *ACS Appl. Mater. Interfaces* **10** 2566